Solid Freeform Fabrication 2022: Proceedings of the 33rd Annual International Solid Freeform Fabrication Symposium – An Additive Manufacturing Conference
Reviewed Paper

Towards directed energy deposition of metals using polymer-based supports: porosity of 316L stainless steel deposited on carbon-fiber-reinforced ABS

Rebecca Kurfess[1,2], Kyle Saleeby[1], Thomas Feldhausen[1], Blane Fillingim[1], A. John Hart[2], David Hardt[2]

[1]Manufacturing Science Division, Oak Ridge National Laboratory, Knoxville, TN
[2]Department of Mechanical Engineering, Massachusetts Institute of Technology, Cambridge, MA

Abstract

Directed energy deposition (DED) is increasingly valuable to many industries because of its high deposition rates relative to other metal additive manufacturing processes, but the design space of DED is limited. For instance, steep overhangs are difficult or impossible to manufacture. Polymer-based support structures could help address this challenge. The viability of DED on polymer composite substrates has begun to be explored, specifically with 316L stainless steel on carbon-fiber-reinforced ABS substrates. Monolithic metal components can be deposited on the polymer, but it was found that gas release during polymer degradation causes porosity due to gas entrapment in the metal. An interlayer cooling time was introduced to reduce polymer degradation and decrease the porosity due to gas entrapment, but this led to porosity from lack of fusion. The results of this work provide insight into process parameter selection and scan strategy development to enable the use of polymer support structures in blown-powder DED.

Keywords: directed energy deposition, support structures, porosity

Introduction

Directed energy deposition (DED) has the capacity to manufacture large, end-use metal components at higher rates compared to other metal additive manufacturing (AM) processes [1, 2]. DED systems use an energy source, usually in the form of a laser or electric arc, to melt either powder or wire metal feedstock as it is being deposited. The design space of all DED additive processes is limited with respect to bridge and overhang capabilities. Keicher et al. patented a DED technology able to manufacture overhangs at or above 60° from the horizontal, while the Stratasys Direct Metal Laser Sintering (DMLS) powder bed fusion process can print overhangs at or above 35° from the horizontal, exemplifying the steeper angle capabilities possible with a powder bed fusion process versus a DED process [3, 4]. Multiple researchers have explored expanding the DED design space by increasing the range of possible overhang angles for DED components. Systems with rotary axes can produce components with steeper overhangs by re-orienting the components during the print [5, 6]. Zhao et al. developed a nonplanar slicing approach to reduce the need for support structures [7]. Lam et al. implemented adaptive process control of a wire-arc DED process to achieve an overhang 52.5° from the horizontal [8]. These results allow for a greater range of overhang angles, but the angles are still limited. Hildreth et al. used multi-material DED printing to create metal support structures out of carbon steel for a stainless steel structure and then dissolved the carbon steel via electrochemical etching [9]. This multi-metal support technology is

promising, but dissolvable metal support structures increase the cost and complexity of the print because of the extra feedstock material required and the etching required during post processing. The support material is limited to metals that will not be etched away during post processing, and the use of a second metal for the supports necessitates an additional powder container the ability for the machine to switch between powder containers during the print.

Polymer support structures for DED components could provide lower-cost, easily-removed supports that would enable steep overhangs and bridges that are currently difficult or impossible to manufacture with DED. There are two key concerns when depositing metal via DED on a polymer structure: the geometric integrity of the polymer and the quality of the deposited metal. If the geometric integrity of the polymer is not maintained due to the polymer melting or degrading, the component cannot be accurately deposited. As DED systems are designed to melt metal, and polymers tend to have degradation temperatures lower than the melting temperatures of most metals, some loss of geometric integrity is to be expected. However, ablative polymers are designed to withstand extreme thermal environments without significant degradation of the polymer, are a potential solution [10]. Assuming that a polymer can be found which can survive the DED process, another concern is the effect of the polymer on the material properties of the metal component. Prior work determined that the use of a carbon-fiber-reinforced ABS substrate for a deposited 316L stainless steel component resulted in an increased hardness of the metal component due to carbon migration from the polymer into the metal [11]. Porosity is also a concern in metal components deposited on polymer substrates. There are two commonly seen types of porosity in metal AM components: lack of fusion defects and gas entrapment porosity, both of which are influenced by print parameters [12]. Lack of fusion defects occur when there is not enough energy from the additive system to fully melt the feedstock material, so some unfused material remains in the final component. Because metal deposition on a polymer substrate requires lowering energy density to avoid significant loss of geometric integrity of the polymer, the energy input might dip below the threshold required for full fusion of the feedstock material. Gas entrapment porosity occurs when gas is introduced into the molten metal and remains trapped inside the component after solidification. Some polymer degradation is expected to occur when the polymer interacts with the energy source and the molten metal, and polymer degradation due to pyrolysis will likely result in the formation of gaseous byproducts [13]. These gases are predicted to become trapped in the metal during deposition, resulting in gas entrapment porosity.

Here, DED of 316L stainless steel on carbon-fiber-reinforced ABS (CF ABS) substrates is performed. Leveraging this capability to understand the effect of using polymer support structures for DED components on the mechanical properties of those components, this research measured the porosity across a 316L stainless steel box structure deposited on CF ABS substrates. Porosity was then measured across a component with an interlayer cooling time added between layers during deposition to determine trends between cooling time, porosity type, and amount of porosity.

Methodology

Substrates of roughly 50mm in length, 25mm in width, and 12.7mm in height were manufactured and mounted in a Haas VF-5/40XT computer numerical control (CNC) system retrofitted by Hybrid Manufacturing Technologies (HMT) with an AMBIT™ S7-2 High Rate Laser Cladding Head for laser blown-powder DED capabilities. Five layers of five 12.7mm-long beads with 0.5mm of overlap between beads were deposited to form a box-shaped geometry with MetcoAdd 316L-D (-106/+45um) stainless steel feedstock powder. The AMBIT™ laser had a spot size of 2mm and the layer height was set to 0.7mm, so the final expected dimensions of the geometry were 12.7mm in length, 8mm in width, and 3.5mm in height, as shown in Figure 1. Deposition settings optimized for 316L stainless steel deposition on stainless steel substrates prior to this work were used, including a laser scan speed of 600mm/min, a shield gas flow of 10L/min, a carrier gas flow rate of 4L/min, and a feedstock powder mass flow rate of 8g/min. Initial testing determined that laser powers above 100W resulted in concerning levels of flaring from the polymer. Because of these safety concerns, laser power, which is usually set between 500W and 750W for stainless steel deposition on stainless steel substrates, was reduced to 100W to address these safety concerns.

Samples were manufactured under two limiting conditions: one with 30 seconds of cooling time programmed at the end of each deposited layer, and one printed continuously with no cooling time. During the cooling time pauses, the laser was turned off, the print head was held in place, and the component was cooled in the printing environment. After printing, the samples were scanned with a ZEISS METROTOM 800 X-Ray computed tomography (XCT) system operating at a tube voltage of 225 kV, tube power of 500W, and a resolution of 6 µm to obtain 3D images of the components and their interiors. The CT results were then analyzed to quantify the porosity of each component. After printing, the samples were mounted, cross sectioned, and polished for microscopic imaging.

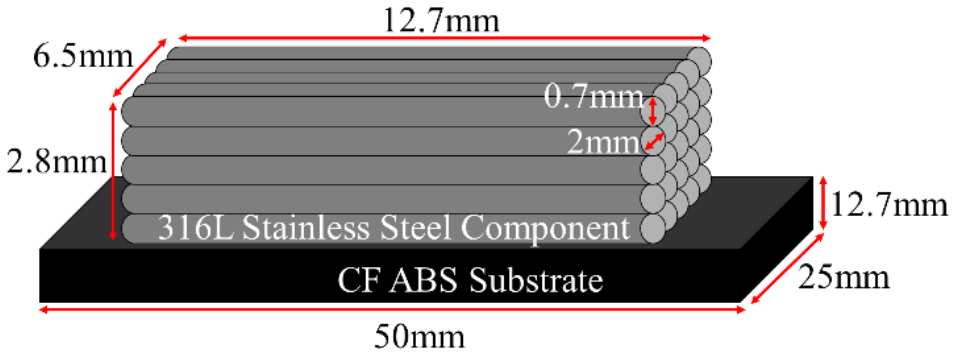

Figure 1: Geometry of 316L stainless steel components printed on CF ABS substrates.

Results and Discussion

The 316L stainless steel components printed with no interlayer cooling time and with 30 seconds of interlayer cooling time are shown in Figure 2. Both components resulted in damage to the CF ABS substrate, particularly the component with no interlayer cooling time. However, the resulting loss of geometric integrity of both substrates were not significant enough to halt the print.

The low laser power in combination with the expected poor surface finish of DED components resulted in some deviations from the expected geometry, although the maximum deviation in each dimension did not exceed up one bead-width, or 2mm. The color on the surface of the component with the 30 second interlayer cooling time indicated some oxidation, while no discoloration was visually observed on the surface of the component with no interlayer cooling time.

No interlayer cooling time

30s interlayer cooling time

Figure 2: 316L stainless steel components printed on CF ABS with no interlayer cooling time (top) and 30 seconds of interlayer cooling time (bottom) [11].

Although both components appear solid and intact, the CT scans and microscopic cross-sectional images shown in Figure 3 reveal substantial porosity. The porosity in the component with no interlayer cooling is mainly rounded and smooth in appearance, indicating that the porosity in this component is dominated by gas entrapment porosity. These pores formed when degradation of the polymer substrate produced gaseous byproducts that infiltrated the molten steel during the print. The porosity in the component with a 30 second interlayer cooling time is jagged, and pores are mainly located between beads. These characteristics indicate that the porosity in this component is dominated by lack of fusion defects, which are due to the low power used during deposition in combination with the interlayer cooling time, which prevented heat buildup in the component.

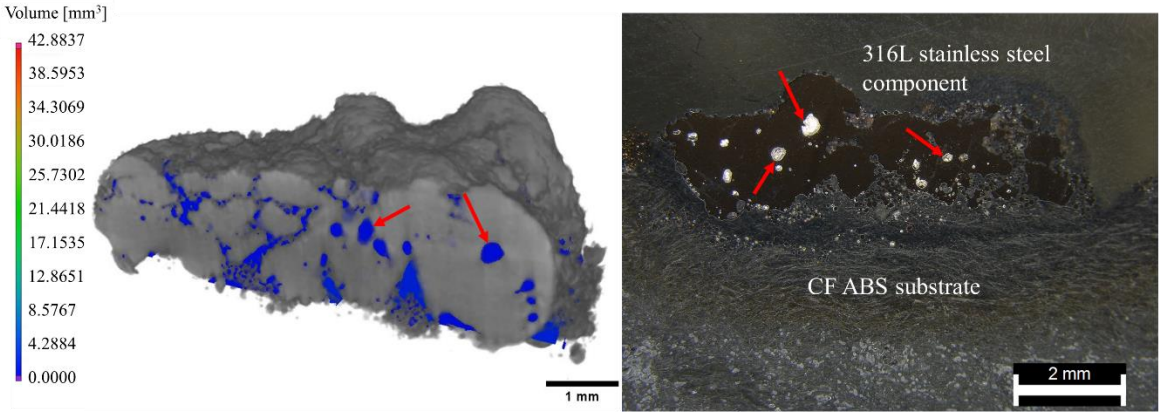

No interlayer cooling time

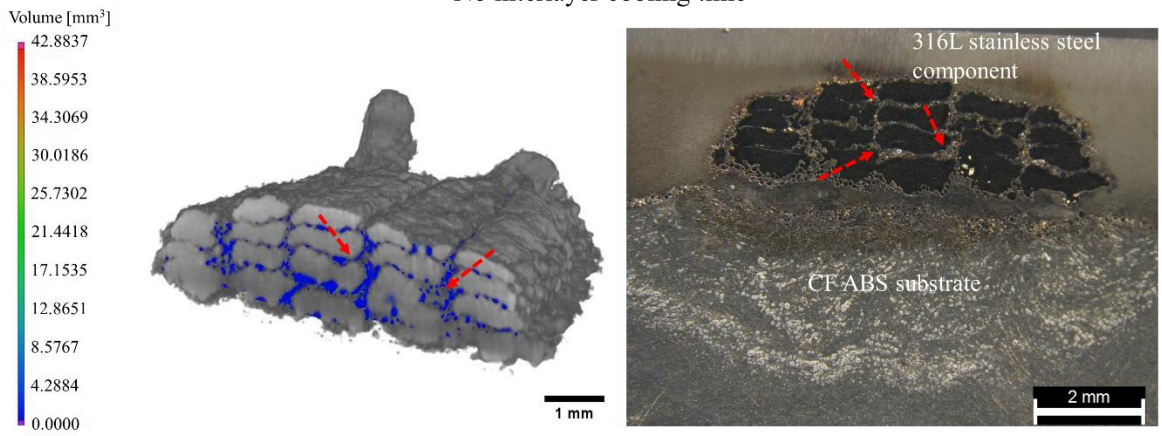

30s interlayer cooling time

Figure 3: CT scans and microscopic cross-sectional images of 316L stainless steel components printed on CF ABS with no interlayer cooling time (top), with solid arrows indicating porosity due to gas entrapment, and 30 seconds of interlayer cooling time (bottom), with dashed arrows indicating porosity due to lack of fusion.

The CT data was then used to analyze the sphericity and diameter of the pores in each component. The results of this analysis are shown in Figure 4, which plots the diameter versus the sphericity of each pore in the component with no interlayer cooling time (top) and the component with a 30 second interlayer cooling time (bottom). The pores in the component with no interlayer cooling time tended to be larger and slightly less spherical than the pores in the component with a 30 second interlayer cooling time. This is consistent with the observation that porosity in the component with no interlayer cooling time is the result of gas entrapment due to gaseous byproduct of polymer degradation infiltrating the melted metal. Porosity in the component with a 30 second interlayer cooling time, on the other hand, is predominantly caused by lack of fusion defects, which cause more jagged pores due to the energy input into the feedstock powder not being large enough to fully melt the material prior to part solidification.

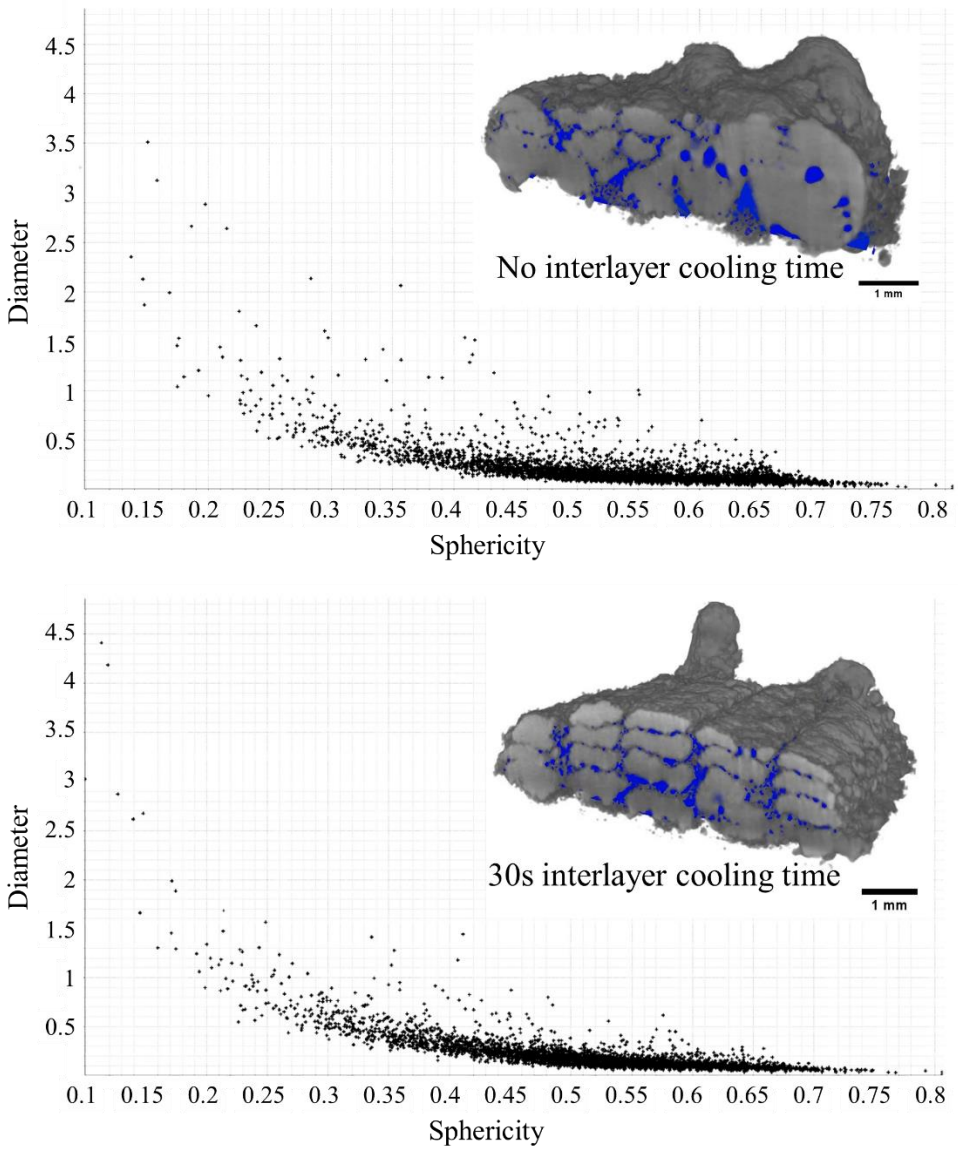

Figure 4: Pore diameter versus sphericity of 316L stainless steel components printed on CF ABS with no interlayer cooling time (top) and 30 seconds of interlayer cooling time (bottom)

The porosity was also quantitatively measured in each component, calculating the ratio of pores to total volume. The porosity of the component with no interlayer cooling time was found to be 8.25%, and the porosity of the component with a 30 second interlayer cooling time was found to be 4.49%. The difference in these porosity values indicates that porosity due to gas entrapment is a greater concern during the first several layers of a metal component deposited on a polymer substrate. Therefore, an interlayer cooling time, which prevents heat buildup and reduces polymer degradation, is desirable for these first few layers. However, after enough metal layers are deposited to insulate the component from gas infiltration, the interlayer cooling time should be reduced or eliminated to reduce porosity due to lack of fusion.

Conclusion

CF ABS was used as a substrate material to deposit 316L stainless steel box structures with different interlayer cooling times to determine the effect of using a polymer substrate in the DED process on the porosity of the deposited component. The porosity of the component with no interlayer cooling time was dominated by gas entrapment porosity, as gas produces during polymer pyrolysis infiltrated the melted feedstock material and remained trapped during solidification. The porosity of the component with a 30 second interlayer cooling time was dominated by lack of fusion defects, as the cooling time prevented heat buildup and therefore decreased the energy available to melt the feedstock material. The tradeoff between porosity types should be considered when designing toolpaths for metal components deposited on polymer substrates. For the first several layers, gas entrapment porosity will dominate, and an interlayer cooling time should be introduced to prevent this porosity. Although this will result in lack of fusion defects, the porosity due to lack of fusion defects will be less than the porosity due to gas entrapment without an interlayer cooling time. After several layers, this interlayer cooling time can be eliminated to prevent lack of fusion defects, as the component will be protected from gas infiltration by the solidified layers. Future research should include a wider range of cooling times to quantify the tradeoffs between cooling time and porosity, as well as developing print strategies to minimize porosity during metal deposition on polymer substrates.

Acknowledgements

The authors acknowledge the cooperation and support of Hybrid Manufacturing Technologies, as well as Dennis Brown, Sarah Graham, and Ryan Duncan. This manuscript is based upon work supported by the U.S. Department of Energy, Office of Energy Efficiency and Renewable Energy, Advanced Manufacturing Office under contract number DE-AC05-00OR22725.

Bibliography

[1] "VC-500A/5x AM HWD." [Online]. Available: https://www.mazakusa.com/machines/vc-500a-5x-am-hwdfiles/375/vc-500a-5x-am-hwd.html.

[2] "Metal Binder Jetting," (in en-US), *Digital Alloys*, 2019/07/11/T14:11:23-04:00 2019. [Online]. Available: https://www.digitalalloys.com/blog/binder-jetting/files/427/binder-jetting.html.

[3] "Design Guidelines: Direct Metal Laser Sintering (DMLS)." [Online]. Available: https://www.stratasysdirect.com/resources/design-guidelines/direct-metal-laser-sintering-old

[4] D. M. Keicher, J. L. Bullen, P. H. Gorman, J. W. Love, K. J. Dullea, and M. E. Smith, "Forming structures from CAD solid models," ed: Google Patents, 2002.

[5] L. Yuan *et al.*, "Application of multidirectional robotic wire arc additive manufacturing process for the fabrication of complex metallic parts," *IEEE Transactions on Industrial Informatics*, vol. 16, no. 1, pp. 454-464, 2019.

[6] J. S. Panchagnula and S. Simhambhatla, "A Novel Methodology to Manufacture Complex Metallic Sudden Overhangs in Weld-Deposition Based Additive Manufacturing," 2021.
[7] G. Zhao, G. Ma, J. Feng, and W. Xiao, "Nonplanar slicing and path generation methods for robotic additive manufacturing," *The International Journal of Advanced Manufacturing Technology*, vol. 96, no. 9, pp. 3149-3159, 2018/06/01 2018, doi: 10.1007/s00170-018-1772-9.
[8] T. F. Lam, Y. Xiong, A. G. Dharmawan, S. Foong, and G. S. Soh, "Adaptive process control implementation of wire arc additive manufacturing for thin-walled components with overhang features," *The International Journal of Advanced Manufacturing Technology*, pp. 1-11, 2019.
[9] O. J. Hildreth, A. R. Nassar, K. R. Chasse, and T. W. Simpson, "Dissolvable metal supports for 3D direct metal printing," *3D Printing and Additive Manufacturing*, vol. 3, no. 2, pp. 90-97, 2016.
[10] M. Favaloro, "Ablative Materials," in *Kirk-Othmer Encyclopedia of Chemical Technology*.
[11] R. Kurfess, R. Kannan, T. Feldhausen, K. Saleeby, A. J. Hart, and D. Hardt, "Towards directed energy deposition of metals using polymer-based supports: hardness of 316L stainless steel deposited on carbon-fiber-reinforced ABS," in *Accepted to ASME 2022 17th International Manufacturing Science and Engineering Conference*, 2022.
[12] G. Ng, A. Jarfors, G. Bi, and H. Zheng, "Porosity formation and gas bubble retention in laser metal deposition," *Applied Physics A*, vol. 97, no. 3, pp. 641-649, 2009.
[13] R. E. Lyon, "Pyrolysis kinetics of char forming polymers," *Polymer Degradation and Stability*, vol. 61, no. 2, pp. 201-210, 1998.